NEUROSCIENCE

Microglia-mediated degradation of perineuronal nets promotes pain

Shannon Tansley[1,2], Ning Gu[1], Alba Ureña Guzmán[1], Weihua Cai[1], Calvin Wong[1], Kevin C. Lister[1], Einer Muñoz-Pino[3], Noosha Yousefpour[4], R. Brian Roome[5], Jordyn Heal[1], Neil Wu[1], Annie Castonguay[3], Graham Lean[6], Elizabeth M. Muir[7], Artur Kania[5,8], Masha Prager-Khoutorsky[6], Ji Zhang[9,10,11], Christos G. Gkogkas[12], James W. Fawcett[13,14], Luda Diatchenko[1,10,11], Alfredo Ribeiro-da-Silva[4,8,11], Yves De Koninck[3,4,11], Jeffrey S. Mogil[1,2,11]*, Arkady Khoutorsky[1,10,11]*

Activation of microglia in the spinal cord dorsal horn after peripheral nerve injury contributes to the development of pain hypersensitivity. How activated microglia selectively enhance the activity of spinal nociceptive circuits is not well understood. We discovered that after peripheral nerve injury, microglia degrade extracellular matrix structures, perineuronal nets (PNNs), in lamina I of the spinal cord dorsal horn. Lamina I PNNs selectively enwrap spinoparabrachial projection neurons, which integrate nociceptive information in the spinal cord and convey it to supraspinal brain regions to induce pain sensation. Degradation of PNNs by microglia enhances the activity of projection neurons and induces pain-related behaviors. Thus, nerve injury–induced degradation of PNNs is a mechanism by which microglia selectively augment the output of spinal nociceptive circuits and cause pain hypersensitivity.

P eripheral nerve injury leads to long-lasting pain hypersensitivity. Damaged primary afferents release chemokines, signaling molecules, and proteases to activate spinal cord microglia, which in turn enhance the excitability of spinal nociceptive circuits (1, 2). Microglia release an array of bioactive substances that bind to cell surface receptors to increase neuronal activity through modulation of intracellular processes (1, 2). How these substances specifically sensitize pain-processing circuits without affecting other modalities is not well understood. Studies of mechanisms by which microglia affect neuronal functions in the spinal cord have focused on intracellular mechanisms of action rather than modulation of the extracellular matrix. The extracellular matrix in the central nervous system (CNS) not only provides structural support but is also involved in the regulation of neuronal excitability and synaptic plasticity (3, 4). Its role in the regulation of spinal pain circuits, however, remains ill defined. Perineuronal nets (PNNs) are the most prominent extracellular matrix structures in the CNS and are composed of a proteoglycan core protein decorated by chondroitin sulfate sugar chains (3). In the neocortex, PNNs preferentially enwrap neuronal soma and proximal dendrites of fast-spiking parvalbumin-positive inhibitory interneurons (5), modulating their potential for neuroplasticity by regulating synaptic inputs (6) and intrinsic excitability (7). We investigated whether PNNs are found around and affect the activity of spinal cord neurons involved in the processing of nociceptive information.

PNNs in lamina I surround projection neurons

PNNs can be identified by staining with *Wisteria floribunda* agglutinin (WFA), which selectively binds the glycosaminoglycan (GAG) sugar side chains of PNN glycoproteins. Additionally, PNNs can be visualized by labeling their core protein component, aggrecan (3, 8, 9). Immunostaining of spinal cord sections for aggrecan showed that PNNs surround neurons with large-diameter soma in lamina I of the dorsal horn that exhibit a medio-lateral orientation (Fig. 1A). High-resolution confocal Airyscan imaging revealed presynaptic inhibitory terminals located within PNN holes (Fig. 1, B and C). Retrograde tracing with Fluoro-Gold (FG) injected into the lateral parabrachial (LPb) nucleus showed that PNNs in lamina I are present selectively around spinoparabrachial projection neurons (10, 11) and not found around other cell types (Fig. 1, D and E). Lamina I PNN-positive (PNN$^+$) projection

neurons have significantly larger soma than those of PNN-negative (PNN$^−$) projection neurons, or other neuronal cell types (volumetric values are provided in Fig. 1F, and soma diameters are provided in fig. S1A), and are NK1R$^+$ and Phox2a$^−$ (fig. S1, B to E). PNNs are absent in lamina II and are sparsely found throughout lamina III of the dorsal horn (Fig. 1A). In laminae IV and V, PNNs are found around both inhibitory (Pax2$^+$) and excitatory (Pax2$^−$ and NeuN$^+$) neurons (Fig. 1A). Exposure of mouse hind paw to mechanical (25-g binder clip for 30 s) (Fig. 1, G and I) or thermal (55°C water bath for 30 s) (Fig. 1, H and I) noxious stimuli induced Fos expression in PNN$^+$ lamina I projection neurons (thermal stimuli, in 70.6 ± 1.7% of neurons; mechanical stimuli, in 49.3 ± 5.2% of neurons), suggesting that these neurons are involved in the processing of pain-related information.

Modification of PNNs after peripheral nerve injury

To study whether PNNs in the spinal cord are modified after peripheral nerve injury, we subjected mice to the spared nerve injury (SNI) assay of neuropathic pain, which features pain behaviors at maximal levels by 2 to 3 days after injury (12, 13). The intensity of WFA staining, which labels GAGs on PNNs (Fig. 1J), around lamina I projection neurons was significantly reduced 3 days after SNI (decrease of 76.3%) (Fig. 1, K and L), whereas aggrecan staining was not affected. WFA staining around lamina I projection neurons remained low at 7 and 14 days after nerve injury (Fig. 1L). PNNs in deeper laminae did not show a decrease in WFA staining (fig. S1, F and G).

PNN degradation is mediated by microglia

Three days after SNI, numerous microglia contained WFA immunoreactivity within their lysosomes, identified by means of labeling with antibody to CD68 (Fig. 2A). Microglia showing CD68 and WFA colocalization were present at day 3 after SNI (67.1% of all microglia in the dorsal horn) (Fig. 2, A and B; sex-disaggregated analysis is available in fig. S1, H, I, and J) but not at later time points (days 7 and 14). To study the causal role of microglia in the degradation of PNNs after nerve injury, we depleted microglia using Cre-inducible mice expressing diphtheria toxin receptor (DTR) (14) selectively in microglia (iDTR;TMEM119^{CreERT2}) (the treatment regimen with tamoxifen to induce Cre expression and diphtheria toxin to ablate microglia is provided in Fig. 2C, and the effect on microglia is provided in Fig. 2D) (15). Peripheral nerve injury in microglia-depleted mice did not evoke mechanical hypersensitivity (Fig. 2E: sex-disaggregated analysis is available in fig. S1K) and did not induce degradation of PNNs because no significant reduction in WFA signal around lamina I projection neurons was observed at day 3 after SNI (Fig. 2, F and G).

[1]Department of Anesthesia, McGill University, Montreal, QC, Canada. [2]Department of Psychology, Faculty of Science, McGill University, Montreal, QC, Canada. [3]Department of Psychiatry and Neuroscience, CERVO Brain Research Centre, Université Laval, Québec, QC, Canada. [4]Department of Pharmacology and Therapeutics, McGill University, Montreal, QC, Canada. [5]Institut de Recherches Cliniques de Montreal (IRCM), Montreal, QC, Canada. [6]Department of Physiology, McGill University, Montreal, QC, Canada. [7]Department of Physiology, Development and Neuroscience, University of Cambridge, Cambridge, UK. [8]Department of Anatomy and Cell Biology, McGill University, Montreal, QC, Canada. [9]Department of Neurology and Neurosurgery, McGill University, Montreal, QC, Canada. [10]Faculty of Dental Medicine and Oral Health Sciences, Montreal, QC, Canada. [11]Alan Edwards Centre for Research on Pain, McGill University, Montreal, QC, Canada. [12]Biomedical Research Institute, Foundation for Research and Technology-Hellas, University Campus, 45110 Ioannina, Greece. [13]John van Geest Centre for Brain Repair, Department of Clinical Neurosciences, University of Cambridge, Cambridge, UK. [14]Centre for Reconstructive Neuroscience, Institute for Experimental Medicine CAS, Prague, Czech Republic.
*Corresponding author. Email: jeffrey.mogil@mcgill.ca (J.S.M.); arkady.khoutorsky@mcgill.ca (A.Kh.)
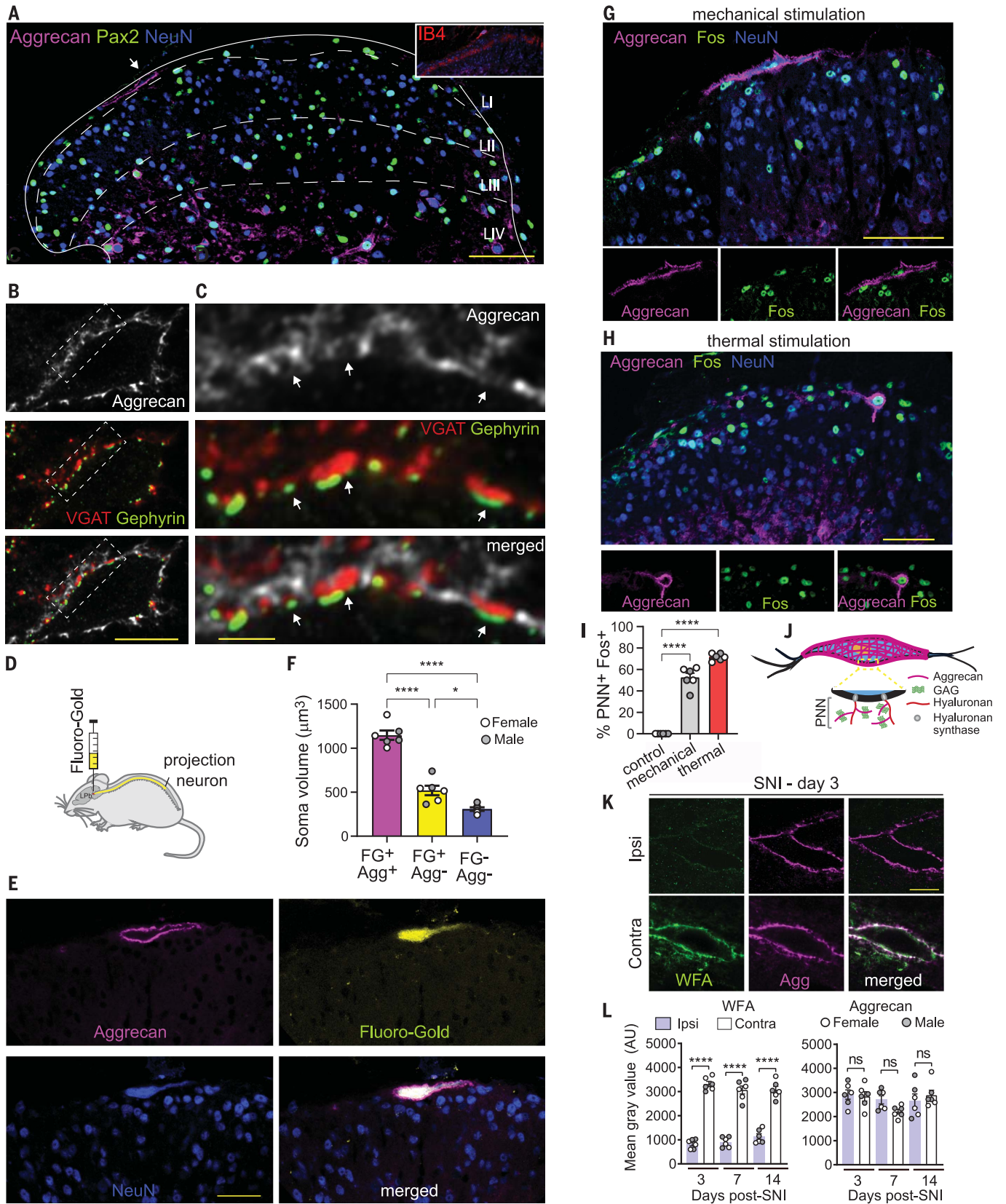
Fig. 1. PNNs are found around lamina I projection neurons and are modified after peripheral nerve injury. (**A**) Immunostaining for a marker of inhibitory neurons (Pax2), all neurons (NeuN), and aggrecan. PNNs are present around large-diameter neurons in lamina I (white arrow). Scale bar, 100 µm.

(**B**) Low-magnification and (**C**) high-magnification Airyscan images. VGAT labels presynaptic inhibitory terminals; gephyrin labels postsynaptic inhibitory compartment. Scale bars, (B) 10 µm; (C) 2 µm. (**D**) Schematic illustration showing retrograde labeling of spinoparabrachial projection neurons in a mouse injected

with FG into the LPb nucleus. (**E**) Immunostaining against aggrecan shows that lamina I projection neurons are retrogradely labeled by FG. (**F**) Lamina I projection neurons surrounded by PNNs (Agg⁺) have larger soma volume than those of PNN-negative projection neurons or other cell types [FG⁺ Agg⁺ versus FG⁺ Agg⁻, $q(15) = 13.8$, $P < 0.0001$; FG⁺ Agg⁺ versus FG⁻ Agg⁻, $q(15) = 18.5$, $P < 0.0001$; $n = 6$ mice per group, one-way analysis of variance (ANOVA) followed by Tukey's post-hoc comparison]. (**G** and **H**) Images of Fos expression after (G) mechanical and (H) thermal stimuli. Scale bar, 100 μm. (**I**) Quantification of the percentage of lamina I PNN⁺ projection neurons showing Fos immuno-reactivity 60 min after the evoking mechanical and thermal stimuli. Each data

point represents one animal ($n = 6$ per condition). (**J**) Schematic showing different components of PNNs. (**K**) Staining with WFA for GAG shows elimination of GAGs from PNNs at day 3 after SNI. Scale bar, 10 μm. (**L**) Quantification of WFA (left) and aggrecan (right) signal around lamina I projection neurons at day 3, day 7, and day 14 after SNI shows reduced WFA signal but no change in aggrecan levels [WFA, day 3 Ipsi versus Contra, $q(30) = 20.5$, $P < 0.0001$; day 7 Ipsi versus Contra, $q(30) = 17.8$, $P < 0.0001$; day 14 Ipsi versus Contra, $q(30) = 15.93$, $P < 0.0001$; one-way ANOVA followed by Tukey's post-hoc comparison, $n = 6$ mice per condition]. All data are presented as mean ± SEM. *$P < 0.05$; ****$P < 0.0001$; ns, not significant.
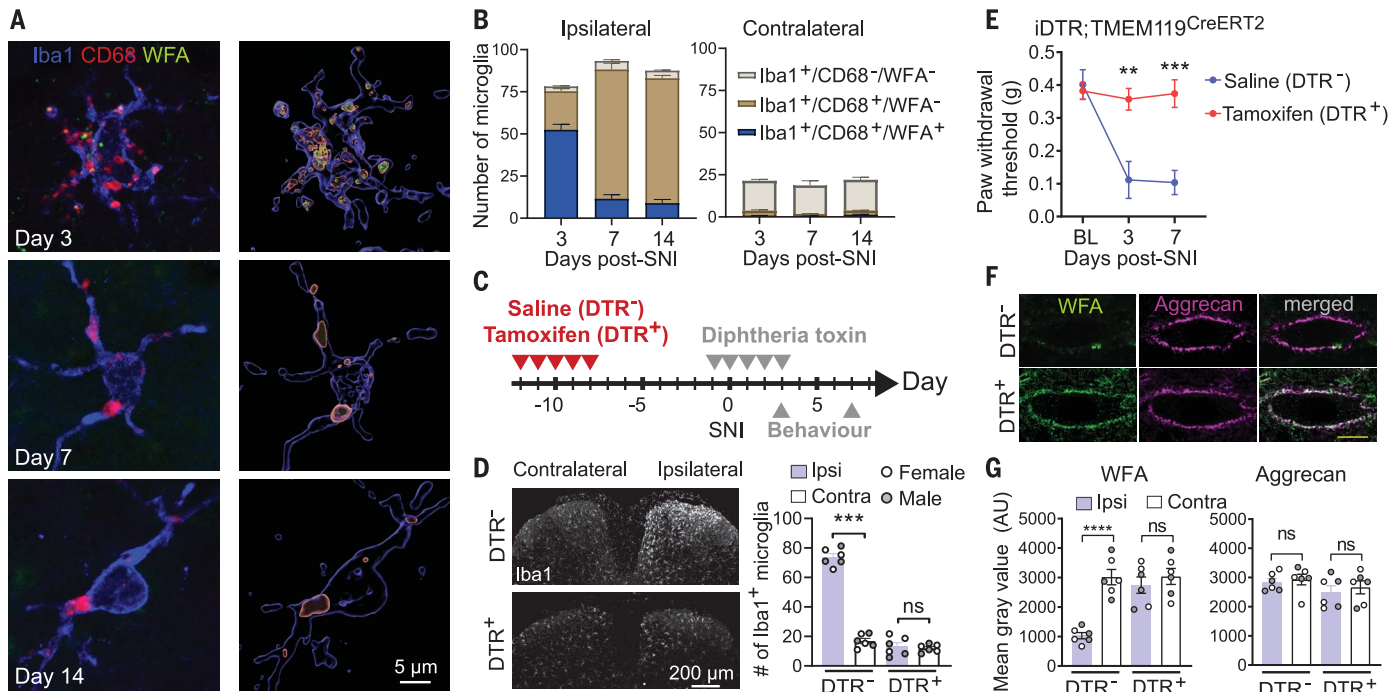
Fig. 2. Microglia mediate the degradation of PNNs around lamina I projection neurons. (**A**) (Left) Microglia (Iba1), lysosomes (CD68), and GAG (WFA) at day 3, day 7, and day 14 after SNI in the dorsal horn spinal cord. (Right) Reconstruction with Imaris software. (**B**) Quantification of the number of microglia per section with and without CD68 and WFA in the dorsal horn ($n = 6$ mice per condition). (**C**) Protocol for administration of tamoxifen and diphtheria toxin (DT) in iDTR;TMEM119^CreERT2 mice. (**D**) Images showing Iba1⁺ microglia in saline-treated (DTR⁻, control) and tamoxifen-treated (DTR⁺, microglia-depleted) iDTR;TMEM119^CreERT2 mice (both groups received DT). Quantification on the right shows the number of microglia in both groups ($n = 6$ mice per group, one-way ANOVA followed by Tukey's post-hoc comparison). (**E**) SNI in microglia-depleted

mice does not lead to the development of mechanical hypersensitivity as assessed with von Frey filaments [withdrawal threshold: day 3, DTR⁻ versus DTR⁺, $t(66) = 4.241$, $P = 0.001$; day 7, DTR⁻ versus DTR⁺, $t(66) = 4.7$, $P = 0.0002$; $n = 12$ mice per group, two-way ANOVA followed by Sidak's post-hoc comparison]. Images (**F**) and quantification (**G**) showing elimination of GAGs from PNNs in control mice but not in microglia-depleted mice on day 3 after SNI [WFA, DTR⁻, Ipsi versus Contra, $q(20) = 8.3$, $P < 0.0001$; DTR⁺, Ipsi versus Contra, $q(20) = 1,22$, $P = 0.82$; $n = 6$ mice per condition, one-way ANOVA followed by Tukey's post-hoc comparison]. Scale bar, 10 μm. All data are presented as mean ± SEM. **$P < 0.01$, ***$P < 0.001$, ****$P < 0.0001$; ns, not significant.

To further corroborate the role of microglia in the modification of PNNs, we used mice lacking CX3C chemokine receptor 1 (CX3CR1) (*16*), which is involved in microglia activation and stimulation of their phagocytic activity (*17–19*). After peripheral nerve injury, *Cx3cr1*⁻ᐟ⁻ mice showed microgliosis comparable with that of control animals (fig. S2, A and B) but exhibited a significantly reduced number of microglial lysosomes (identified with CD68 immunostaining) (fig. S2, C and D), indicating reduced phagocytic activity. *Cx3cr1*⁻ᐟ⁻ mice also did not develop pain hypersensitivity (fig. S2E), which is con-

sistent with previous reports (*20*). Nerve injury in *Cx3cr1*⁻ᐟ⁻ animals did not trigger PNN degradation around lamina I projection neurons (fig. S2, F and G), similarly to that in microglia-depleted mice, and significantly reduced WFA accumulation was detected in microglia at day 3 after SNI (fig. S2, C, H, and I).

Disruption of PNNs around projection neurons promotes pain-related behavior

To study whether the removal of PNNs around projection neurons can induce pain, we deleted aggrecan in projection neurons by injecting

Acan^fl/fl mice (*8*) with adeno-associated virus-retro (rAAV2)–Cre into the LPb nucleus (Fig. 3A). rAAV2-Cre allows retrograde labeling and expression of Cre recombinase in neurons projecting to the LPb (*21*, *22*), including lamina I spinoparabrachial projection neurons (characterization of rAAV2-Cre is available in fig. S3). We validated the disruption of PNNs around lamina I projection neurons in rAAV2-Cre–injected *Acan*^fl/fl mice (Fig. 3, B and C). The elimination of PNNs around spinoparabrachial projection neurons caused thermal hypersensitivity; latencies to paw-licking and
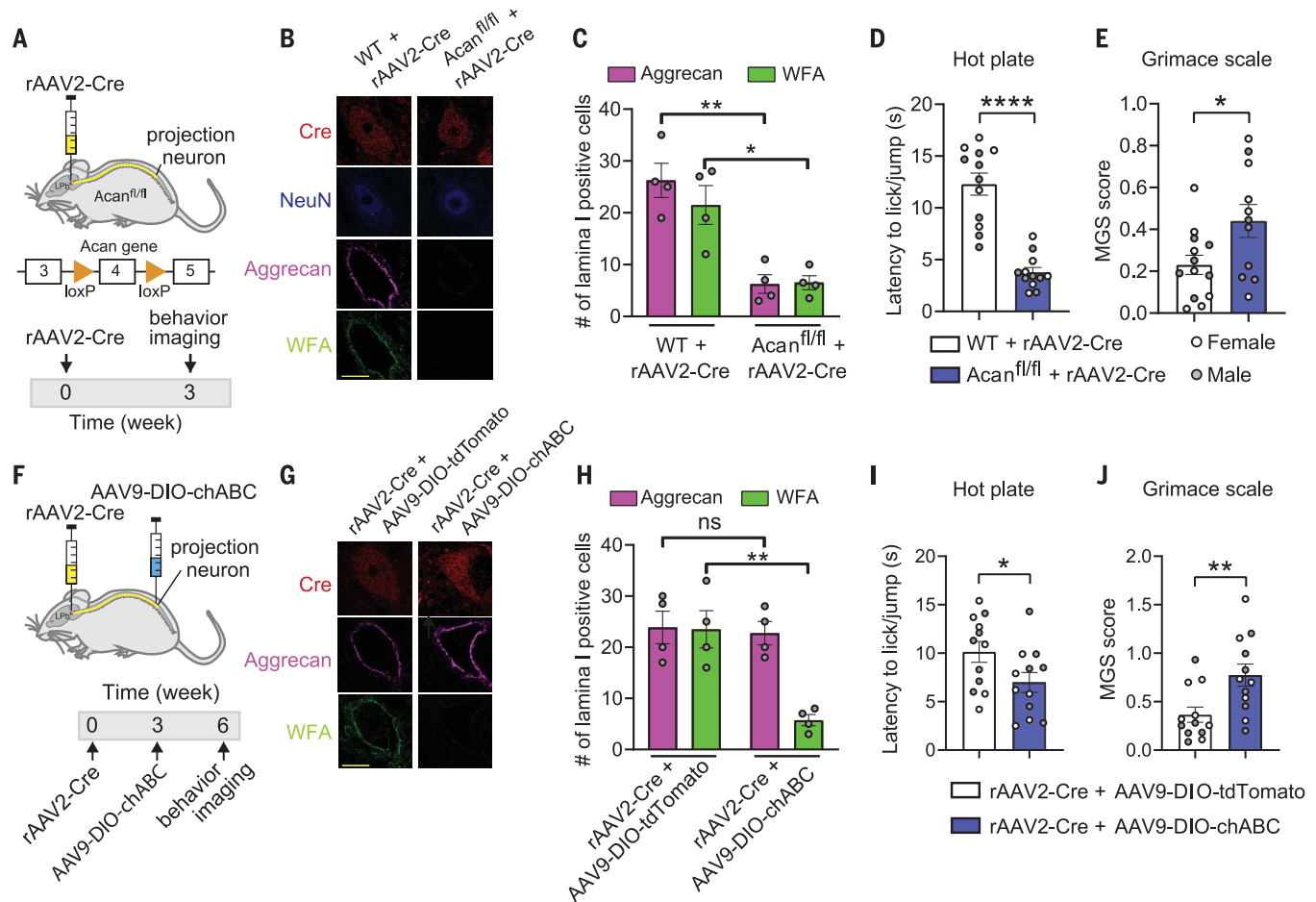
Fig. 3. Selective disruption of PNNs around lamina I projection neurons causes pain. (**A**) Schematic illustration showing the injection of rAAV2-Cre into the LPb nucleus of Acan^fl/fl mice. (**B**) Lamina I spinoparabrachial projection neurons, identified by staining against Cre. (**C**) Quantification of aggrecan+ and WFA+ cells in lamina I of the lumbar spinal cord [aggrecan, wild type (WT) + rAAV2-Cre versus Acan^fl/fl + rAAV2-Cre, $q(12) = 7.3$, $P = 0.0012$; WFA, WT + rAAV2-Cre versus Acan^fl/fl + rAAV2-Cre, $q(12) = 5.5$, $P = 0.01$; $n = 4$ mice per condition, one-way ANOVA followed by Tukey's post-hoc comparison]. (**D** and **E**) Control and aggrecan-ablated mice were subjected to (D) hot plate and (E) Mouse Grimace Scale testing. Mice with ablation of aggrecan in lamina I spinoparabrachial projection neurons exhibit reduced time to licking and jumping in the hot plate test [(D) WT + rAAV2-Cre ($n = 12$ mice) versus Acan^fl/fl + rAAV2-Cre ($n = 12$ mice), $P < 0.0001$; unpaired t test] and increased facial expressions of pain [(E) WT + rAAV2-Cre ($n = 13$ mice) versus Acan^fl/fl + rAAV2-Cre ($n = 11$ mice), $P = 0.03$; unpaired Student's t test].

(**F**) chABC was expressed in lumbar spinoparabrachial projection neurons by means of coinjection of rAAV2-Cre into the LPb nucleus and Cre-dependent AAV9-DIO-chABC into the lumbar spinal cord. (**G**) Cre-expressing neurons show reduced WFA signal but no change in aggrecan levels. (**H**) Quantification of aggrecan+ and WFA+ cells in lamina I of the lumbar spinal cord [aggrecan: $q(12) = 0.411$, $P = 0.991$, WFA: $q(12) = 6.5$, $P = 0.003$; $n = 4$ mice per condition, one-way ANOVA followed by Tukey's post-hoc comparison]. (**I** and **J**) Mice expressing chABC in projection neurons show (I) reduced latency in the hot plate test [rAAV2-Cre + AAV9-DIO-tdTomato ($n = 12$ mice) versus rAAV2-Cre + AAV9-DIO-chABC ($n = 12$ mice); $P = 0.046$, unpaired Student's t test] and (J) increased spontaneous pain measured by the Mouse Grimace Scale [rAAV2-Cre + AAV9-DIO-tdTomato ($n = 12$ mice) versus rAAV2-Cre + AAV9-DIO-chABC ($n = 12$ mice); $P = 0.008$, unpaired Student's t test]. All data are presented as mean ± SEM. *$P < 0.05$; **$P < 0.01$; ****$P < 0.0001$; ns, not significant. Scale bar, 10 μm.

jumping in the hot plate test were significantly shortened in Acan^fl/fl mice injected with rAAV2-Cre as compared with control animals (Fig. 3D). Removal of PNNs also elicited spontaneous pain as assessed with the Mouse Grimace Scale (Fig. 3E). Because peripheral nerve injury decreases GAGs on PNNs without affecting aggrecan (Fig. 1, L and M), and a limitation of the previous approach that all neurons projecting to the LPb nucleus are targeted, we next mimicked the effect of nerve injury on PNNs by selectively removing GAGs around lumbar spinal cord projection neurons by using adeno-associated virus (AAV)–

expressing chondroitinase ABC (chABC) (23). ChABC specifically digests GAGs on PNNs and has been extensively used to study the role of PNNs in the nervous system (6, 24, 25). Expression of chABC in projection neurons in lumbar spinal cord was achieved by co-injecting two viral vectors: rAAV2-Cre into the LPb nucleus, and AAV-expressing chABC in a Cre-dependent manner (AAV9-DIO-chABC) into the lumbar spinal cord (Fig. 3F). This approach resulted in the removal of GAGs from lamina I PNNs without affecting aggrecan (Fig. 3, G and H). It did not change PNNs in deeper laminae (fig. S4A) or cause microglia activation (fig.

S4B). Removal of GAGs from lumbar spinal cord projection neurons induced thermal hypersensitivity in the hot plate test (Fig. 3I) and evoked spontaneous pain in the Mouse Grimace Scale (Fig. 3J).

Removal of GAG disinhibits lamina I projection neurons

Previous studies in the cortex and hippocampus have revealed that PNNs regulate synaptic transmission (25) and affect intrinsic neuronal excitability (7). Our finding of PNN degradation promoting pain behavior (Fig. 3) prompted us to investigate whether removal of PNN GAGs
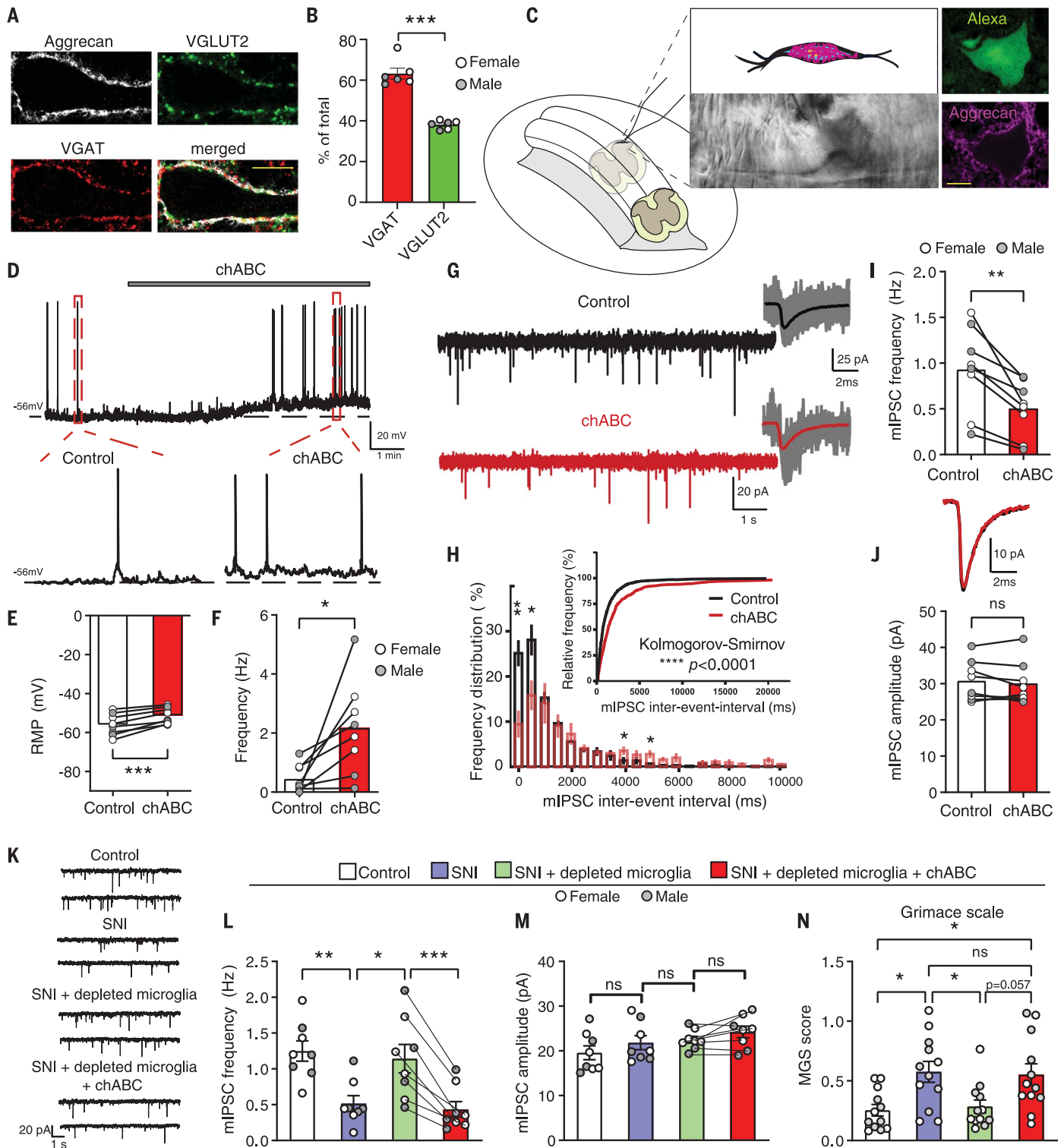
Fig. 4. Removal of PNNs increases projection neurons activity through disinhibition. (**A**) Immunostaining against presynaptic inhibitory (VGAT) and excitatory (VGLUT2) terminal markers around the cell body of PNN+ lamina I projection neuron. (**B**) Quantification of (A) (P < 0.0001, n = 6 mice per condition, unpaired Student's t test). (**C**) Whole-cell recording in ex vivo spinal cord from large-diameter (>20 μm) lamina I neurons showing mediolateral orientation, which have PNNs. These cells were identified by use of oblique infrared illumination with LED. To verify the presence of PNNs around the patched cells, Alexa fluor 488 hydrazide was added to the patch electrode,

followed by fixation and immunostaining for aggrecan. 82% of patched cells were positive for aggrecan (images on the right). (**D** to **F**) Current clamp recording shows that treatment with chABC induces membrane potential depolarization [(D) and (E), P = 0.00055, n = 8 cells from eight mice per group] and an increase in firing rate [(D) and (F), P = 0.022, n = 8 cells from eight mice per group, paired Student's t test]. (**G**) mIPSCs before and after treatment with chABC (0.2 U/ml for 10 min). (**H**) Frequency distribution histogram. (**I** and **J**) The frequency of mIPSCs is reduced after chABC treatment [(I) P = 0.003], but the mIPSC amplitude is not [(J) P = 0.69, n = 8 cells from eight mice per group,

paired Student's *t* test]. (**K** to **M**) mIPSC recorded from lamina I PNN⁺ neurons in sham (control), SNI (3 to 5 days after surgery), SNI+depleted microglia (tamoxifen-treated iDTR;TMEM119^CreERT2 mice+DT), and SNI+depleted microglia+chABC (chABC applied onto ex vivo spinal cord) mice (*n* = 8 cells from eight mice per group, one-way ANOVA followed by Tukey's post-hoc comparison for the three first columns, paired Student's *t* test for the last two columns).

(**N**) Mouse Grimace Scale testing on control, SNI (SNI+vehicle), SNI+depleted microglia (SNI+PLX5622+rAAV2-Cre+AAV9-DIO-tdTomato), and SNI+depleted microglia+chABC (SNI+PLX5622+rAAV2-Cre+AAV9-DIO-chABC, *n* = 12 animals per group, one-way ANOVA) (a detailed timeline is available in the supplementary materials, materials and methods). All data are presented as mean ± SEM. *$P <$ 0.05; **$P <$ 0.01; ***$P <$ 0.001; ns, not significant. Scale bar, 10 μm.

increases the activity of lamina I projection neurons in the dorsal horn of the spinal cord.

First, we assessed the number of excitatory and inhibitory synaptic inputs onto PNN⁺ projection neurons by quantifying inhibitory [vesicular γ-aminobutyric acid transporter–positive (VGAT⁺)] and excitatory [vesicular-glutamate transporter 2–positive (VGLUT2⁺)] presynaptic puncta (Fig. 4A). Significantly more VGAT⁺ than VGLUT2⁺ puncta (60% more) were present on the soma of PNN⁺ projection neurons (Fig. 4B). Elimination of GAGs from PNNs by injecting AAV-chABC into the lumbar spinal cord did not change the number of excitatory and inhibitory presynaptic terminals on PNN⁺ projection neurons (fig. S5, A and B). The number of excitatory and inhibitory presynaptic terminals also remained unchanged 3 days after SNI (fig. S5, C and D).

To study the impact of GAG removal on neuronal activity of lamina I projection neurons, we measured synaptic inputs into these neurons and their intrinsic excitability using whole-cell patch-clamp recording in an ex vivo spinal cord preparation (Fig. 4C) (26). Large-diameter (>20 μm) lamina I neurons with mediolateral orientation, which are surrounded by PNNs (fig. S1A), were identified in intact spinal cord for patch clamp recording by using oblique infrared illumination with a light-emitting diode (LED) (27). To confirm the presence of PNNs around these neurons, we filled the patched cells with Alexa fluor 488 hydrazide, followed by fixation and aggrecan immunostaining (Fig. 4C). Degradation of GAG with chABC resulted in a depolarization of membrane potential (4.8 ± 1 mV) (Fig. 4, D and E) and an increase in action potential firing rate (Fig. 4, D and F). This effect was specific to neurons with PNNs because chABC did not change membrane potential and firing rate in PNN⁻ neurons (fig. S5E). Analysis of spontaneous miniature synaptic activity revealed that chABC decreased the frequency of miniature inhibitory postsynaptic currents (mIPSCs) (48% decrease) (Fig. 4, G, H, and I) but not their amplitude (Fig. 4, G and J). No effects on the frequency or amplitude of miniature excitatory postsynaptic currents (mEPSCs) were detected (fig. S6, A to C). Moreover, degradation of PNNs had no effect on passive membrane properties and intrinsic excitability of projection neurons in the presence of synaptic receptor antagonist cocktail (AP-5, DNQX, bicuculline, and strychnine) to suppress both excitatory and inhibitory synaptic

activities (fig. S6, D to M). To confirm that disruption of PNNs after nerve injury is accompanied by a decrease in inhibitory inputs, we recorded from lamina I PNN⁺ projection neurons on day 3 after SNI and found a significant reduction in the frequency of mIPSCs (Fig. 4, K to M). This reduction was prevented in mice with depletion of microglia (iDTR; TMEM119^CreERT2) but could be reinstated through removal of PNNs with chABC. Consistent with these results, nerve injury–induced spontaneous pain was alleviated by depletion of microglia (by using the CSF1R inhibitor PLX5622) but was reinstated through removal of PNNs around lamina I projection neurons (Fig. 4N).

Discussion

We have uncovered a mechanism by which activated microglia selectively augment the output of spinal nociceptive circuits and thus evoke pain. A subpopulation of lamina I spino-parabrachial projection neurons are preferentially surrounded by PNNs, which are degraded after peripheral nerve injury in a microglia-dependent manner (fig. S7). Degradation of PNNs is sufficient to enhance projection neuron activity, through reduction of inhibitory synaptic inputs, and to promote pain behaviors.

Whereas in the cortex and hippocampus, PNNs are largely found around parvalbumin interneurons (28), in the dorsal horn of the spinal cord, PNNs are found in lamina I exclusively around large-diameter projection neurons and surround various neuronal types in deeper laminae. The selective localization of PNNs around projection neurons, but not other cell types in the superficial dorsal horn, allows for regulation of projection neuron activity, by means of modulation of PNNs, with a high degree of specificity. Because projection neurons are the main output of spinal pain circuits, activation of projection neurons through degradation of PNNs around them is a specific and efficient mechanism to augment the output of spinal nociceptive circuits.

Synaptic terminals are embedded in PNNs, and thus the composition and stability of PNNs have a profound impact on synaptic activity (5, 25). Removal of GAGs that bear negatively charged sulfate groups on PNNs might result in destabilization of synaptic structures and reduce the efficiency of synaptic transmission. Future studies will be required to obtain a better mechanistic understanding of the effect of PNN degradation on inhibitory synapses around projection neurons.

Microglia play crucial roles in the promotion of pain states through several known mechanisms (1, 2). Reduction of inhibitory tone—through microglia-mediated down-regulation of the K⁺-Cl⁻ cotransporter (KCC2), resulting in increased intracellular chloride and attenuated inhibitory inputs—promotes neuropathic pain (29). Down-regulation of KCC2 and chloride dysregulation occur in several cell types in lamina I and II at day 7 after nerve injury (30, 31). Microglia-mediated degradation of PNNs selectively augments the activity of a subset of lamina I projection neurons and is observed at 3 days after injury. The existence of several microglia-dependent processes to promote pain that might act in parallel with different cellular specificity and temporal profiles reflects the complexity and robustness of mechanisms underlying neuropathic pain and suggests that efficient treatments should target several processes to reverse hypersensitivity.

Sex differences in the involvement of microglia in mediating chronic pain have been demonstrated (32, 33), although microgliosis occurs equally in both sexes after nerve injury (32, 33), and not all pain models (34) and elements of the spinal signaling pathway (30) are sexually dimorphic. We found that microglia-dependent degradation of PNNs and its effect on synaptic activity and pain-related behavior is present in both males and females.

Neuronal activity promotes the formation and maintenance of PNNs around parvalbumin-positive neurons (35). It remains to be determined how enhanced activity of spinal circuits after peripheral nerve injury affects the dynamics of PNNs around lamina I projection neurons, including their recovery from degradation and long-term maintenance.

Our work uncovers a mechanism by which microglia disinhibit projection neurons after peripheral nerve injury. These findings might lead to the development of therapeutic strategies to reverse neuropathic pain by targeting this newly discovered mechanism.

REFERENCES AND NOTES

1. M. W. Salter, B. Stevens, *Nat. Med.* **23**, 1018–1027 (2017).
2. G. Chen, Y. Q. Zhang, Y. J. Qadri, C. N. Serhan, R. R. Ji, *Neuron* **100**, 1292–1311 (2018).
3. J. W. Fawcett, T. Oohashi, T. Pizzorusso, *Nat. Rev. Neurosci.* **20**, 451–465 (2019).
4. H. H. Shen, *Proc. Natl. Acad. Sci. U.S.A.* **115**, 9813–9815 (2018).
5. E. Favuzzi et al., *Neuron* **95**, 639–655.e10 (2017).
6. T. Pizzorusso et al., *Science* **298**, 1248–1251 (2002).
7. K. K. Lensjø, M. E. Lepperød, G. Dick, T. Hafting, M. Fyhn, *J. Neurosci.* **37**, 1269–1283 (2017).
8. D. Rowlands et al., *J. Neurosci.* **38**, 10102–10113 (2018).
9. D. Carulli et al., *J. Comp. Neurol.* **494**, 559–577 (2006).

10. R. Wercberger, A. I. Basbaum, *Curr. Opin. Physiol.* **11**, 109–115 (2019).
11. C. Peirs, R. Dallel, A. J. Todd, *J. Neural Transm.* **127**, 505–525 (2020).
12. I. Decosterd, C. J. Woolf, *Pain* **87**, 149–158 (2000).
13. S. D. Shields, W. A. Eckert3rd, A. I. Basbaum, *J. Pain* **4**, 465–470 (2003).
14. T. Buch *et al.*, *Nat. Methods* **2**, 419–426 (2005).
15. T. Kaiser, G. Feng, *eNeuro* **6**, ENEURO.0448-18.2019 (2019).
16. S. Jung *et al.*, *Mol. Cell. Biol.* **20**, 4106–4114 (2000).
17. S. Lee *et al.*, *Am. J. Pathol.* **177**, 2549–2562 (2010).
18. M. K. Zabel *et al.*, *Glia* **64**, 1479–1491 (2016).
19. G. Milior *et al.*, *Brain Behav. Immun.* **55**, 114–125 (2016).
20. A. A. Staniland *et al.*, *J. Neurochem.* **114**, 1143–1157 (2010).
21. D. G. Tervo *et al.*, *Neuron* **92**, 372–382 (2016).
22. A. G. J. Skorput *et al.*, *PLOS ONE* **17**, e0264938 (2022).
23. J. N. Alves *et al.*, *J. Neurosci. Methods* **227**, 107–120 (2014).
24. E. J. Bradbury *et al.*, *Nature* **416**, 636–640 (2002).
25. A. Dityatev, M. Schachner, P. Sonderegger, *Nat. Rev. Neurosci.* **11**, 735–746 (2010).
26. P. Szucs, L. L. Luz, D. Lima, B. V. Safronov, *J. Comp. Neurol.* **518**, 2645–2665 (2010).
27. P. Szucs, V. Pinto, B. V. Safronov, *J. Neurosci. Methods* **177**, 369–380 (2009).
28. C. Peirs, R. P. Seal, *Science* **354**, 578–584 (2016).
29. J. A. Coull *et al.*, *Nature* **424**, 938–942 (2003).
30. J. C. S. Mapplebeck *et al.*, *Cell Rep.* **28**, 590–596.e4 (2019).
31. K. Y. Lee, S. Ratté, S. A. Prescott, *eLife* **8**, e49753 (2019).
32. R. E. Sorge *et al.*, *Nat. Neurosci.* **18**, 1081–1083 (2015).
33. S. Taves *et al.*, *Brain Behav. Immun.* **55**, 70–81 (2016).
34. J. Peng *et al.*, *Nat. Commun.* **7**, 12029 (2016).
35. G. Devienne *et al.*, *J. Neurosci.* **41**, 5779–5790 (2021).

ACKNOWLEDGMENTS

SUPPLEMENTARY MATERIALS

science.org/doi/10.1126/science.abl6773
Materials and Methods
Figs. S1 to S7
References (*36–45*)
MDAR Reproducibility Checklist

View/request a protocol for this paper from *Bio-protocol*.

Science

Microglia-mediated degradation of perineuronal nets promotes pain

Shannon TansleyNing GuAlba Ureña GuzmánWeihua CaiCalvin WongKevin C. ListerEiner Muñoz-PinoNoosha YousefpourR. Brian RoomeJordyn HealNeil WuAnnie CastonguayGraham LeanElizabeth M. MuirArtur KaniaMasha Prager-KhoutorskyJi ZhangChristos G. GkogkasJames W. FawcettLuda DiatchenkoAlfredo Ribeiro-da-SilvaYves De KoninckJeffrey S. MogilArkady Khoutorsky

Microglia can cause chronic pain

Peripheral nerve injury leads to long-lasting pain hypersensitivity. Treatment of chronic pain continues to be unsatisfactory because we still don't fully understand the underlying processes. Tansley *et al.* discovered a new mechanism by which peripheral nerve injury causes pain. A subpopulation of projection neurons in the spinal cord dorsal horn that are critical for transmission of pain signals to the brain, but not other cell types in superficial dorsal horn, are selectively surrounded by specialized extracellular matrix structures called perineuronal nets. Nerve injury–activated microglia degrade perineuronal nets around projection neurons, which increases projection neuron activity, subsequently causing pain. —PRS

View the article online
https://www.science.org/doi/10.1126/science.abl6773
Permissions
https://www.science.org/help/reprints-and-permissions

Use of this article is subject to the Terms of service